Optimizing Thermal Insulation of Cir-Q: A Study on Mycelium-Composite Filling for Sustainable Building Components

Chen Hou 0834661

Statement for Using AI

I used ChatGPT to provide various forms of assistance with my writing, including:

- Revising Sentences and Paragraphs: Assisting in making sentences and paragraphs clearer and more academic.
- Rephrasing and Replacing Terms: Offering guidance on rephrasing specific terms and replacing words to improve accuracy and coherence.
- Shortening Long Sentences: Helping to break down long sentences into shorter, more easy-reading ones.
- RStudio Code Assistance: Providing support in writing and debugging RStudio code for data analysis.

Optimizing Thermal Insulation of Cir-Q: A Study on Mycelium-Composite Filling for Sustainable Building Components

A research internship by

Chen Hou, student number 0834661
Faculty of Science, Utrecht Universit, Utrecht, the Netherlands
Contact: c.hou1@students.uu.nl

Supervised by

Prof. dr. H.A.B. Wösten
Faculty of Science, Molecular Microbiology, Utrecht University, Padualaan 8, 3584 CH, Utrecht, the Netherlands
Contact: H.A.B.Wösten@uu.nl

Roland van Driel
First Circular Insulation, Blaak 34, 3011 TA Rotterdam, the Nethetlands
Contact: r.vandriel@fc-i.com

Hans Borra
Comfordak, Kritzingerlaan 61, 3707 TB Zeist, the Netherlands
Contact: borra@comfortdak.nl

Examiners

Dr. L.G. (Luis) Lugones
Faculty of Science, Molecular Microbiology, Utrecht University, Padualaan 8, 3584 CH, Utrecht, the Netherlands
Contact: l.g.lugones@uu.nl

This research internship is an assignment within the master program Bio Inspired Innovation of Utrecht University, the Netherlands.

Utrecht, March 2024 – August 2024

Contents

Abstract

Mycelium composites are an emerging and novel biomaterial with significant potential to replace petrochemical-based insulation for more energy-efficient buildings. These materials offer comparable thermal insulation while being more sustainable, 100% circular, and less energy-intensive. This research centers on optimizing the thermal insulation properties of Cir-Q, a sustainable building component designed by FC-i in collaboration with Comfortdak. Cir-Q consists of mycelium composites used as insulation fillings, encased in oriented strand board (OSB) for structural support.

The current production method involves a sawing-then-compressing strategy, where dried and shaped mycelium composites are compressed into OSB cases, aiming to eliminate gaps between the mycelium material and the OSB. However, the challenge lies in controlling the degree of compression to avoid increasing the material's thermal conductivity. This research addressed two main objectives: first, to test and compare the thermal insulation properties of two mycelium composites produced by FC-i, both derived from the same fungal species *G. lucidum* but cultivated on different substrates; second, to conduct compression experiments on the materials, measuring changes in density and thermal conductivity before and after different levels of compression, as well as assessing the rebound capability of the materials to predict the optimal compression rate for mycelium fillings.

The results of this study indicated that the two mycelium composites (0.0539- 0.0666 W/Mk) did not show significant differences in their thermal insulation properties, though both were lower than those of commonly used insulation materials. Notably, the study found that when the materials were mildly compressed by 10% or 20%, their thermal conductivity slightly decreased rather than increased, and the materials demonstrated excellent rebound performance, stabilizing within three days with no observed shrinkage. Additionally, even when compressed 40% or 50% of their original volume, the thermal insulation properties of the materials did not change statistically, while their compressive strength significantly improved. Furthermore, it was noted that as the mycelium composites were compressed, the thermal conductivity initially decreased, reaching a minimum point, then began to increase as density continued to rise. This trend was explained by possible changes in the porosity and pore size within mycelium composites during compression.

These findings offer promising prospects for the further development of Cir-Q products.

Keywords: Mycelium composites, Insulation materials, Thermal conductivity, Compression, Resilience

Layman’s summary

Mycelium composites are an innovative and eco-friendly material made by growing fungi on agricultural waste like wood and grass fibers. These materials have the potential to replace traditional insulation in buildings, offering similar thermal insulation while being more sustainable and less energy-intensive. This research focuses on improving the insulation properties of Cir-Q, a building component developed by FC-i and Comfortdak. Cir-Q uses mycelium composites as insulation, which are enclosed in oriented strand board (OSB) for structural support.

The current production method involves a sawing-then-compressing strategy, where dried and shaped mycelium composites are compressed into OSB cases, aiming to eliminate gaps between the mycelium material and the OSB. However, the challenge lies in controlling the degree of compression to avoid increasing the material's thermal conductivity since the density will increase after compression. This research addressed two main objectives: first, to test and compare the thermal insulation properties of two mycelium composites produced by FC-i, both derived from the same fungal species *G. lucidum* but cultivated on different substrates; second, to conduct compression experiments on the materials, measuring changes in density and thermal conductivity before and after different levels of compression, as well as assessing the rebound capability of the materials to predict the optimal compression rate for mycelium fillings.

The results of this study indicated that the two mycelium composites (0.0539- 0.0666 W/Mk) did not show significant differences in their thermal insulation properties, though both were lower than those of commonly used insulation materials. Notably, the study found that when the materials were mildly compressed by 10% or 20%, their thermal conductivity slightly decreased rather than increased, and the materials demonstrated excellent rebound performance, stabilizing within three days with no observed shrinkage. Additionally, even when compressed 40% or 50% of their original volume, the thermal insulation properties of the materials did not change statistically, while their compressive strength significantly improved. Furthermore, it was noted that as the mycelium composites were compressed, the thermal conductivity initially decreased, reaching a minimum point, then began to increase as density continued to rise. This trend was explained by possible changes in the porosity and pore size within mycelium composites during compression.

These findings offer promising prospects for the further development of Cir-Q products.

1. Introduction

Construction is the largest consumer of energy globally, and the processing of raw materials for buildings as well as their construction puts enormous pressure on natural resources and the environment (Hung Anh & Pásztory, 2021). Energy used to heat and cool buildings accounts for close to one-third of the total global energy consumption, and adding insulation to the building envelope can effectively reduce building energy consumption and improve energy efficiency (Sutcu, 2015; X. Zhang, Hu, Fan, & Yu, 2022).

Currently, the most widely used insulation materials in the market are inorganic materials such as glass wool or rock wool, because of their good insulation properties, fire resistance, and resistance to moisture (Hung Anh & Pásztory, 2021). However, it can cause health issues such as skin and lung irritation (Hung Anh & Pásztory, 2021). In addition, organic materials such as polyurethane (PUR), polyisocyanurate (PIR), extruded polystyrene (XPS), expanded polystyrene (EPS) with low thermal conductivity and low cost are used as insulation materials (Villasmil, Fischer, & Worlitschek, 2019). However, the production of these synthetic and petroleum-based materials consumes large amounts of energy and non-renewable resources, creates a large carbon footprint, and may release hazardous substances that are harmful to health during use. Moreover, most of these synthetic materials are non-biodegradable, generating large amounts of waste that pollutes the environment at the end of their life (Dias, Jayasinghe, & Waldmann, 2021; Girometta et al., 2019; X. Zhang et al., 2022).Therefore, it has been necessary to seek more eco-friendly and renewable insulation materials to build more sustainable buildings.

A growing number of studies in recent years have shown that fungal mycelium composites have the potential to be the bio-alternatives of synthetic and petroleum-based materials (Girometta et al., 2019; Jones, Mautner, Luenco, Bismarck, & John, 2020). Mycelium composite is achieved by growing the fungus in a substrate, often agricultural waste such as hemp shives, straw, sawdust, rice hulls and corn cobs (Bitting et al., 2022; van den Brandhof & Wösten, 2022). The colonization of fungi as a low-energy biomanufacturing method produces a biodegradable lightweight material that can replace energy-intensive synthetic materials (Jones et al., 2020). During growing, the mycelium of the fungus acts as a natural adhesive to cement the substrate matrix and a part of the substrate is gradually replaced by the mycelium biomass (Girometta et al., 2019; Jones et al., 2020).

Mycelium composites offer superior material properties such as good thermal insulation, high acoustic absorption and fire safety properties. (Jones et al., 2020). Additionally, they are totally biobased and biodegradable (Angelova, Brazkova, & Krastanov, 2021). Mycelium materials also have their limitations, such as high moisture uptake, typically foam-like mechanical properties, and low termite resistance (Antinori, Ceseracciu, Mancini, Heredia-Guerrero, & Athanassiou, 2020; Jones et al.,

2020). However, it is undeniable that they show great potential as thermal and acoustic insulation foams. In addition, there is a wide variety of fungi in nature, and the material properties of mycelium materials can be customized according to the composition of the fungal substrate as well as the manufacturing process (Jones et al., 2020), which shows the potential of mycelium materials to be explored and developed.

Figure 1. The prototype of a house made of Cir-Q. The prototype was made by Hans Borra.

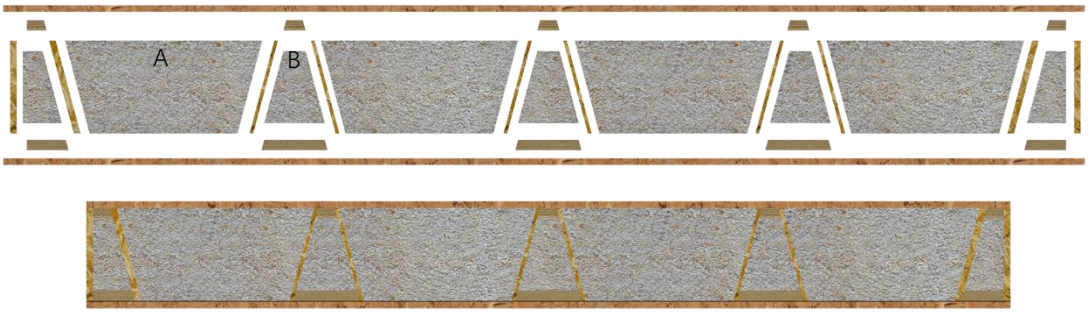

Figure 2. The cross-section view of Cir-Q. A is main filling, B is column filling.

FC-i is a company that leverages the thermal insulation properties of mycelium composites, focusing on the development of organic, fully circular mycelium-based insulators intended to replace petrochemical insulation in energy-efficient buildings. The raw materials for their mycelium composites are sourced from organizations that collect residual streams from the forestry, horticultural, and food production chains (FC-Insulation, 2021). Currently, FC-i is collaborating with Comfortdak to develop a mycelium-based building component known as Cir-Q, designed for use in roofs,

floors, and walls (Figure 1). This product comprises mycelium composites and oriented strand board (OSB). The mycelium composites serve primarily as filler insulation material and are engineered into two irregular trapezoidal forms, referred to as column fillings and main fillings (Figure 2). OSB provides structural support, compensating for the relatively low compressive strength of mycelium materials when compared to traditional building materials such as concrete and wood.

Despite the development of the new product, several challenges persist. One key issue I have been addressing is how to maintain the excellent thermal insulation properties of the mycelium fillings when encased within OSB wood. The initial production method involved cultivating mycelium composites in a trapezoidal mold sized to match the final product dimensions. However, after drying, the mycelium material experienced significant shrinkage due to water loss, resulting in a gap between the mycelium and the mold. This shrinkage poses a twofold problem: first, it undermines the precision of the product's dimensions, hindering further development; second, the gap between the insulation fillings and the OSB can lead to thermal bridging, thereby reducing the overall thermal insulation efficiency of the product.

To address this, the current production approach, Sawing-Compressing strategy, replaces molding with sawing technology to shape the mycelium fillings. In this method, mycelium composites are initially grown in a large square mold. After the growth and drying process, the block of mycelium composite is sawed into the desired trapezoidal shape, slightly larger than the internal volume of the OSB casing. The shaped mycelium fillings are then compressed into the OSB case. We hypothesize that the compressed mycelium will exhibit a slight rebound, ensuring a snug fit within the OSB without any gaps. In this case, the shrinkage of mycelium composites after drying will no longer be an issue. However, this new strategy introduces the challenge of determining the optimal size for the initial mycelium fillings and the appropriate compression distance. Compression increases the density of the mycelium material and reduces its porosity, and since low-density materials typically exhibit lower thermal conductivity, excessive compression could result in higher thermal conductivity in the mycelium (Jones et al., 2020; M. Zhang, Xue, et al., 2023). Therefore, it is crucial to strike a balance between the degree of compression and the thermal insulation properties of the mycelium fillings, ensuring that the final product remains free of gaps and thermal bridging while avoiding any significant increase in thermal conductivity.

Furthermore, the thermal insulation capabilities of mycelium composites are essential when applied in building insulation. The company has measured the thermal conductivity of various mycelium composites, which ranged from 0.040 W/m·K to 0.050 W/m·K, with very occasional values of 0.038 W/m·K. It is notable that the current thermal conductivity of the mycelium fillings of the Cir-Q product remains notably higher compared to conventional insulation materials such as polyurethane (PUR) (0.024-0.03 W/m·K), polyisocyanurate (PIR) (0.018-0.028 W/m·K), extruded polystyrene (XPS) (0.03-0.04 W/m·K), and slightly higher than the commonly used

inorganic insulation materials glass wool (0.03-0.045 W/m·K) and rock wool (0.033-0.045 W/m·K) (Hung Anh & Pásztory, 2021). The company's expectation for the thermal conductivity of the final mycelium fillings is less than 0.032 W/m·K. To achieve this goal and optimize the product's insulating properties, the company plans to experiment with different recipes, such as changing the fungi species, and changing the ratio or type of substrates.

In tackling the above challenges associated with Cir-Q products, the primary objective of my internship research was twofold: 1) Testing and comparing the thermal insulation properties of mycelium composites grown on different substrates. 2) Investigating and predicting the optimal compression rate for mycelium filling to fit in the OSB without gaps and maintaining great thermal insulation properties.

This study involved two distinct potential mycelium composite fillings derived from the same fungal species, *G. lucidum*, but cultivated on different substrates. The thermal conductivity of these composites was assessed using two distinct thermal testing devices. The core of this research was centered around manual compression experiments. In these experiments, samples were subjected to various degrees of compression, and subsequent measurements were taken to analyze changes in density, thermal conductivity, and rebound rate. Additionally, the compressive strength of a subset of samples was evaluated. Ultimately, a comprehensive assessment of the material's thermal insulation performance, rebound capacity, and compressive strength was conducted to propose a potential optimal compression strategy.

2. Materials and methods

2.1. Mycelium composite samples

For this research, three distinct mycelium composites were provided by the FC-i company, as detailed in Table 1. These composites, labeled as A, OB, and B, were all produced using the fungal species *G. lucidum* but were cultivated on different substrates. Sample A was cultivated on a substrate composed of reed, grass, and wood fibers in a ratio of 2:3:5. Both OB and B were grown on a substrate consisting of sawdust, grass, and wood fibers in a ratio of 3:1:6. The key distinction between OB and B is that OB was produced eight months prior to testing. This temporal difference was accounted for in the research to investigate any potential impact on the insulation performance of the material after an extended period.

Table 1. Three samples of mycelium composites were tested, all produced using the same fungal species but cultivated on different substrates. Sample OB was produced eight months prior to the testing dates.

Sample	Fungal species	Substrate

A	*G. Lucidum*	20% reet fibers, 30% grass fibers and 50% wood fibers
OB	*G. Lucidum*	30% sawdust, 10% grass fibers and 60% wood fibers
B		

2.2. Thermal testing and samples preparation

There were two thermal testing devices used in this study: the Heat Flow Meter (HFM-100) (Figure 3.a) and the TEMPOS Thermal Properties Analyzer (METER München) (Figure 3.b). To determine which device was more accurate for measuring thermal conductivity and which was better suited for my experiments, I conducted tests on a range of materials with both devices.

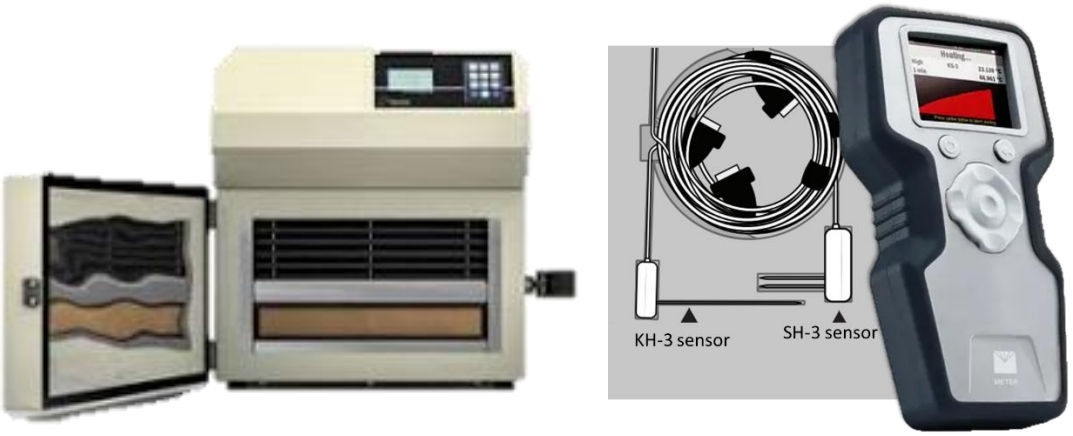

Figure 3. The heat flow meter (HFM-100) (a) and TEMPOS thermal properties analyzer (b).

In addition to the mycelium composites of Sample A and B provided by FC-i, additional mycelium composites and commonly used insulation materials such as rock wool and Styrofoam were also tested using the two thermal testing devices. This broader selection was incorporated to generate a more extensive dataset, allowing for a more robust analysis of the relationship between the thermal conductivity values (λ) obtained from the two devices. Moreover, by comparing the known λ values of rock wool and Styrofoam with the values measured by these devices, the accuracy of each thermal testing device can be assessed.

Prior to thermal testing, the mycelium composites were cut to the required dimensions using a bandsaw machine (Felder FB610) to ensure precision in sample preparation. For the HFM-100 testing, the sample's surface area needed to be larger than 15 cm x 15 cm and smaller than 30 cm x 30 cm to ensure complete coverage of the sensor area located in the center of the upper and lower plates. The maximum permissible sample height was 10 cm, and it was crucial to ensure that the surface of the sample was perfectly flat.

The HFM-100 is user-friendly and primarily operated through computer controls via the Win Test-Analysis EC software. Before initial use, the machine requires calibration using the provided reference material, NIST1450D. The calibration result was saved as a file, which must be loaded before each subsequent measurement. Prior to placing a sample in the machine, the "Zero Plate" function must be activated. Once the zeroing process was complete, the sample was placed in the machine. If the sample was smaller than 30 cm x 30 cm, it was centered on the base plate to fully cover the sensor area ("Heat Flow Meter," 2024). After loading the calibration file, the measurement was initiated. The upper plate automatically lowered to contact the sample's surface and measure its thickness. Each measurement cycle typically took 1-2 hours, after which the thermal conductivity of the sample was determined.

For measurements using the TEMPOS system, the dual-needle SH-3 sensor (35 mm long, 1.3 mm diameter) was inserted into the sample to obtain values for heat capacity. This process was repeated three times on different sides of the sample to ensure accuracy. The mean value of these three measurements was then used as input data when the single-needle KS-3 sensor (60 mm long, 1.3 mm diameter) was inserted into the sample, again repeating the process three times on different sides to determine an average value for thermal conductivity. To minimize errors, it was essential to maintain a minimum of 1.5 cm of material parallel to the sensor in all directions.

2.3. Manual compression experiments

The primary objective of this experiment was to investigate the resilience, density and thermal conductivity changes of mycelium composites after compression. The samples were prepared as follows: each sample was cut into 10 x 10 x 10 cm cubes, derived from three distinct types of mycelium composites labeled A, OB, and B. For each sample type, the samples were divided into groups based on the degree of compression applied, represented by Strain 1, which refers to the intended deformation through compression as a percentage of the original height.

For composite A, a total of 8 samples were used, divided into three groups with $Strain_1$ values of 20%, 30%, and 40%, with 2-3 replicates per group. Similarly, 8 samples of composite OB were divided into two groups with $Strain_1$ values of 20%, 30%, and 50%. Finally, 15 samples of composite B were divided into four groups with Strain 1 values of 10%, 20%, 30%, and 40%.

Before compression, the dimensions (length, width, and height) of each sample were measured. In cases where the sample height was slightly less than 10 cm, the compression distance was adjusted accordingly to ensure consistent compression strain ($Strain_1$) across the same sample group. The samples were then weighed to calculate the initial density, followed by the measurement of the initial thermal conductivity (λ_0). The sample was then placed into a robust, detachable square metal container with internal dimensions of 10 x 10 x 12 cm. A solid square metal block,

designed to fit precisely within the container, was positioned on top of the sample. Vertical compression was applied by manually operating the lever of a compression machine, with the compression distance precisely controlled throughout the process. A ruler was affixed to the machine to accurately determine the compression distance. The compression distance was calculated based on the sample's initial height (h_0) and the target $Strain_1$. For example, for a sample with an initial height of 9.5 cm and a target $Strain_1$ of 20%, the sample would be compressed vertically by 1.9 cm, resulting in a aimed height (h_1) of 7.6 cm. After compressing, the pressure was maintained for 2 minutes before releasing. Although the thermal conductivity at height h_1 could not be measured as the sample tends to rebound immediately upon pressure release, this does not impact the study's objectives.

After removal from the metal container, the sample's height was monitored over time. On the third day, the sample's height (h_2) and weight were measured to calculate the density (ρ_2), and the thermal conductivity (λ_2) was measured. The same measurements were repeated on the 30th day to obtain h_3, ρ_3, and λ_3.

The density and thermal conductivity of the samples before and after compression were then compared to investigate how thermal conductivity changes while density changes and determine the optimal compression rate for the mycelium fillings. Additionally, the rebound rate of each sample was calculated to quantify the material's rebound performance. The rebound rate is defined as the percentage of the distance the sample rebounded from its compressed state (h_1) over three days relative to the initial compression distance. By comparing rebound rates across different samples and groups, the study aimed to assess the material's rebound performance, validating the hypothesis that the mycelium composites would rebound within the OSB cases without forming gaps and thermal bridging.

2.4. Compression testing

Compression testing was carried out on an LS5 materials testing machine (Lloyd Instruments/Ametek, USA) using a 10 kN load cell with a maximum load of 5 kN. The testing protocol included a preload of 5 N at a preload speed of 20 mm/min, with subsequent extension at a rate of 20 mm/min.

RStudio was used for the analysis of raw data, enabling the generation of the stress-strain curve for each composite sample. Compression testing involves the continuous application of pressure until the machine's compression limit is reached. This investigation focused on determining Young's modulus rather than the maximum stress or elongation capacity of the samples. Young's modulus was computed by identifying the point with the highest slope on the stress-strain curve within the 10% - 20% strain range using numerical differentiation.

2.5. Statistics

To evaluate the relationship between density and thermal conductivity, both linear and polynomial regression analyses were performed. Trend lines were fitted to the data, and the coefficient of determination (R^2) was calculated for each model. The R^2 value represents the proportion of variance in thermal conductivity that can be explained by the variance in density within the context of the regression model. A higher R^2 value indicates a better fit of the model to the data, signifying a stronger correlation between the variables.

For each sample type, one-way ANOVA was employed to statistically analyze the density and thermal conductivity of samples across different compression groups, both before and after compression. When the ANOVA revealed significant differences, Tukey's HSD (Honestly Significant Difference) test was subsequently conducted to identify specific differences between two groups. The results of Tukey's HSD test are visualized using the Compact Letter Display (CLD), where groups sharing the same letter are not significantly different, while those with different letters exhibit significant differences. Statistical significance was established with a p-value of ≤ 0.05. Error bars in all figures represent the 95% confidence interval (CI).

To compare only two groups of dependent data, such as the density and thermal conductivity of samples A before and after 20% compression, a paired t-test was utilized to assess if there is a significant difference between these two groups of data tested in different conditions.

3. Results

3.1. Comparing HFM-100 and TEMPOS

In Table 2, λ_1 represents the thermal conductivity measured by the HFM-100, while λ_2 is measured by the TEMPOS. For Sample A, λ_1 is 0.0542 W/m·K , which is more than 1.5 times higher than λ_2. Among the two Sample B variants, the λ_1 of Sample B-1 (0.0539 W/m·K) is significantly lower than that of Sample B-2 (0.0666 W/m·K). However, λ_2 for Sample B-1 (0.0355 ± 0.0041 W/m·K) is slightly higher than that for Sample B-2 (0.0341 ± 0.0016 W/m·K). Consistent with the results for Sample A, the λ_1 values obtained from the HFM-100 are significantly higher across all tested samples compared to the λ_2 values measured by the TEMPOS.

Table 2. Thermal conductivity of the following samples tested by HEM-100 (λ_1) and TEMPOS (λ_2).

Samples		Strain$_1$ (W/m·K)	λ_2 (W/m·K)
A	1	0.0542	0.0344 ± 0.0024
B	1	0.0539	0.0355 ± 0.0041
	2	0.0666	0.0341 ± 0.0016
Mycelium composites	1	0.0620	0.0346 ± 0.0026
	2	0.0602	0.0348 ± 0.0042
	3	0.0614	0.0348 ± 0.0025
Rock wool	1	0.0332	0.0187 ± 0.0015
	2	0.0378	0.0184 ± 0.0004
Expanded Polystyrene (EPS)	1	0.0334	0.0153 ± 0.0001
	2	0.0333	0.0155 ± 0.0004

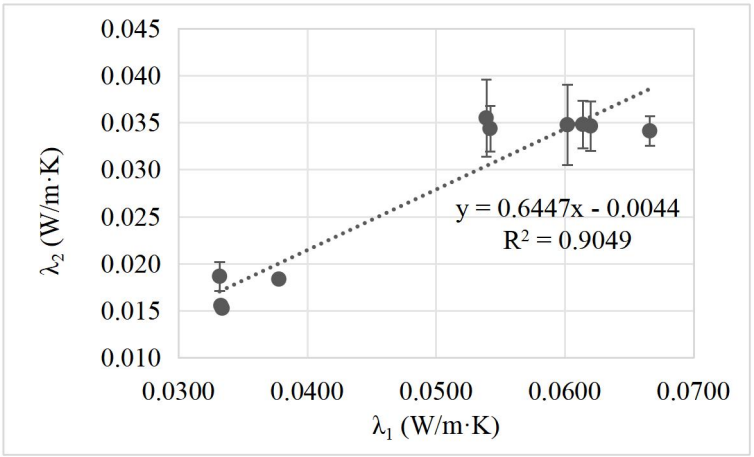

Figure 4. Linear relationship between thermal conductivity measurements obtained with the HFM-100 (λ_1) and the TEMPOS (λ_2) for the same batch of test materials. Error bars represent the 95% confidence interval (CI). R^2 value is the coefficient of determination that represents how well the linear regression model fits the data.

For assessing the potential linear relationship between λ_1 and λ_2, the data presented in Table 1 were plotted in Figure 4. A linear regression analysis was performed on all data points, as illustrated in the figure. The analysis revealed a significant linear correlation between the thermal conductivity values obtained from the HFM-100 and TEMPOS, with a high R^2 of 0.9049.

3.2. Manual compression experiment

To determine the optimal strain (Strain 1) for compressing mycelium fillings into OSB cases without gaps and with minimal reduction in thermal insulation, a manual compression experiment was conducted. This experiment yielded data on the density, thermal conductivity, and rebound rate for three types of samples subjected to various compression rates, as summarized in Table S1 and S2. All thermal tests during this manual compression experiment were performed by TEMPOS.

3.2.1. Investigating the change of density and thermal conductivity after compression

The initial focus was on analyzing the changes in density and thermal conductivity after applying different degrees of compression. Typically, compression increases the material's density, which is often associated with a corresponding increase in thermal conductivity (Jones et al., 2020). Anticipating a linear relationship between these two parameters, the data points for density and the corresponding thermal conductivity for Samples A, OB, and B were plotted in Figure 5. However, the R^2 values for Samples A, OB, and B were 0.0976, 0.5853, and 0.0138, respectively. These low R^2 values indicate that the data from each sample type do not fit well with the linear regression model, suggesting that there is no linear relationship between density and thermal conductivity for any of these three types of mycelium samples.

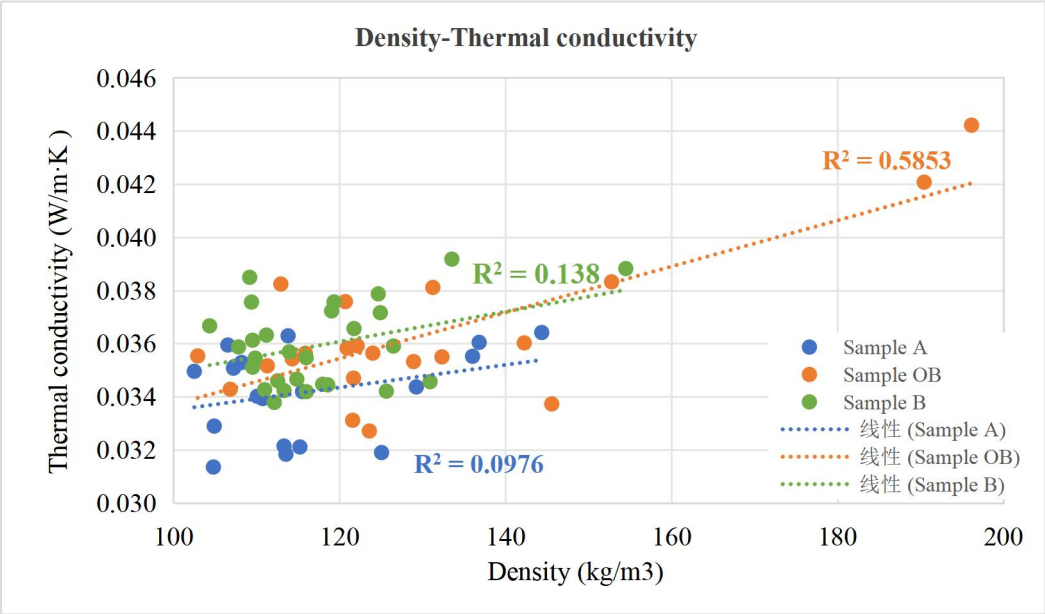

Figure 5. The density and thermal conductivity of all samples, including the three sample types and various compression groups. The three differently colored dashed lines represent the linear regression fit corresponding to each of the three sample types. R^2 value is the coefficient of determination that represents how well the linear regression model fits the data.

After an unsuccessful attempt to establish a linear relationship between the density and thermal conductivity of samples subjected to varying levels of compression, the focus shifted to comparing the effects within the same sample type across different compression levels, as well as before and after compression. As shown in Table 3, the density of Samples A, OB, and B increased progressively with higher levels of compression. However, trends in thermal conductivity varied: for Samples A and OB, thermal conductivity decreased after 20% compression but increased after 30%, 40%, and 50% compression. In contrast, for Sample B, thermal conductivity decreased after 10% compression but increased following 20%, 30%, and 40% compression. To further investigate the changes and relationships among these data groups, one-way ANOVA and Tukey's HSD tests were conducted for different compression levels within the same sample type. Additionally, paired t-tests or t-tests were performed for specific comparisons between two data sets.

Results of one-way Anova and Tukey's HSD testing

The mean densities of each compression group are listed in Table 3a. For Sample A, after three days at 20% compression, the density increased slightly from an initial ρ_0 of 105.42 ± 6.34 kg/m³ to ρ_2 of 112.88 ± 6.45 kg/m³. However, this increase is not statistically significant, as indicated by the shared CLD. Similarly, no significant differences were observed between ρ_3 , measured 30 days after 20% compression, and either ρ_2 or ρ_0. In contrast, densities measured after 30% and 40% compression (ρ_2) showed significant increases compared to all uncompressed samples of Sample A. Additionally, ρ_2 values following 20%, 30%, and 40% compression were significantly

different from each other. For Sample OB, a statistically significant increase in ρ_2 was observed after 50% compression, compared with all uncompressed samples of Sample OB, as well as ρ_2 and ρ_3 measured after 20% compression. Significant differences were also noted between ρ_3 after 50% compression and both the uncompressed Sample OB and ρ_2 after 20% compression. Beyond these findings, no other significant differences were detected within Sample OB. In the case of Sample B, ρ_2 did not increase significantly after 10% compression compared to ρ_0. However, significant increases in density were observed after 20%, 30%, and 40% compression. Furthermore, ρ_2 following 40% compression was significantly higher than in any other group within Sample B.

Table 3. Mean density (a) and mean thermal conductivity (b) of samples before and after varying degrees of compression. *n* represents the number of repetitions in each group. *Strain 1* refers to the applied compressive strain, defined as the ratio of the compressed distance to the original height of the sample. ρ_0 and λ_0 denote the original density and thermal conductivity of the samples before compression. ρ_2 and λ_2 were measured after compression and a 3-day rest period for rebound. ρ_3 and λ_3 were measured 30 days after compression. The CLD labels (a, b, c, etc.) next to the means indicate the results of Tukey's Honest Significant Difference (HSD) test. Within each sample type, means sharing the same letter are not significantly different ($p > 0.05$), while those with different letters are significantly different from each other.

a.

Sample type	Groups		Density (kg/m^3)		
	Strain$_1$ %	n	ρ_0	ρ_2	ρ_3
A	20	3	105.42 ± 6.34 ^{c}	112.88 ± 6.45 ^{c}	113.28 ± 5.98 ^{c}
	30	2	104.85 ± 0.64 ^{c}	127.16 ± 26.62 ^{b}	
	40	3	109.78 ± 8.72 ^{c}	139.07 ± 11.42 ^{a}	
OB	20	3	113.37 ± 5.77 ^{c}	122.1 ± 4.25 ^{c}	122.47 ± 2.48 ^{bc}
	30	3	114.02 ± 17.51 ^{c}	134.51 ± 17.21 ^{abc}	
	50	2	117.08 ± 179.98 ^{c}	174.46 ± 275.53 ^{a}	168.01 ± 285.06 ^{ab}
B	10	3	107.68 ± 7.18 ^{c}	111.12 ± 3.38 ^{c}	
	20	6	114.56 ± 4.23 ^{c}	124.24 ± 5.27 ^{b}	
	30	3	110.75 ± 5.53 ^{c}	125.83 ± 18.1 ^{b}	
	40	3	114.82 ± 10.29 ^{bc}	155.96 ± 10.8 ^{a}	

b.

Sample type	Groups		Thermal conductivity (W/(m·K))		
	Strain$_1$ %	n	λ_0	λ_2	λ_3
A	20	3	0.0353 ± 0.0013 ^{ab}	0.0328 ± 0.0027 ^{bc}	0.0333 ± 0.0032 ^{abc}
	30	2	0.0321 ± 0.0098 ^{c}	0.0331 ± 0.0157 ^{abc}	
	40	3	0.0356 ± 0.0016 ^{ab}	0.036 ± 0.0011 ^{a}	
OB	20	3	0.0363 ± 0.0041	0.0354 ± 0.0056	0.0344 ± 0.004
	30	3	0.0352 ± 0.002	0.0356 ± 0.0009	
	50	2	0.0368 ± 0.0164	0.0413 ± 0.0375	0.0379 ± 0.053

B	10	3	0.0371 ± 0.0031^{abc}	0.0348 ± 0.0015^{c}	
	20	6	0.0346 ± 0.0007^{c}	0.0358 ± 0.0014^{bc}	
	30	3	0.0356 ± 0.0043^{abc}	0.0379 ± 0.0028^{ab}	
	40	3	0.0365 ± 0.0024^{abc}	0.0385 ± 0.0019^{a}	

Regarding thermal conductivity, as presented in Table 3b, no significant differences were observed between the groups for Sample OB with the result of one-way Anova test($p=0.18$. For Sample A, the mean thermal conductivity values before (λ_0) and after (λ_2) compression showed no significant differences across 20%, 30%, and 40% compression levels. However, λ_0 in the 30% compression group was statistically distinct from λ_0 in the other two groups. Additionally, λ_2 measured after 40% compression was significantly higher compared to λ_2 measured after 20% compression. In Sample B, significant differences were observed only between λ_2 after 40% compression and λ_2 measured after both 10% and 20% compressions. Besides, λ_2 following 10% compression also differed significantly from λ_2 measured after 30% compression.

Results of pair t-test and t-test

The pairwise t-test results for pre- and post-compression data largely align with the findings from Tukey's HSD test. However, additional insights emerged when performing t-tests across different sample types. Specifically, the density and thermal conductivity of the uncompressed original samples B and OB were not significantly different, with p-values of 0.582 and 0.543, respectively. In contrast, significant differences in density were observed between the uncompressed original Samples A and OB ($p = 0.046$), although their thermal conductivity values were not significantly different. Similar findings were noted when comparing Samples A and B. Moreover, there were no statistically significant differences in either density or thermal conductivity between Sample B and Sample OB after 20% and 30% compression.

In summary, the findings from Table 3 and data statisticly anylysis indicate the following: 1) The density and thermal conductivity of Samples A, OB, and B did not exhibit statistically significant differences between pre- and post-compression states at 10% or 20% compression, even though mean thermal conductivity appeared to decrease while density increased. 2) The density of Sample A with 20% and 30% compression, Sample OB with 50% compression, and Sample B with 20%, 30%, and 40% compression showed statistically significant increases compared to pre-compression values. However, the thermal conductivity did not exhibit statistically significant differences after compression. 3) For Samples A and OB, density and thermal conductivity measurements taken 30 days after compression showed slight changes compared to measurements taken 3 days after compression, but these differences were not statistically significant. 4) No significant differences in thermal conductivity were found between Samples A, OB, and B. 5) There were no significant differences in either density or thermal conductivity between Sample B and Sample OB, regardless of whether the samples were tested before or after compression.

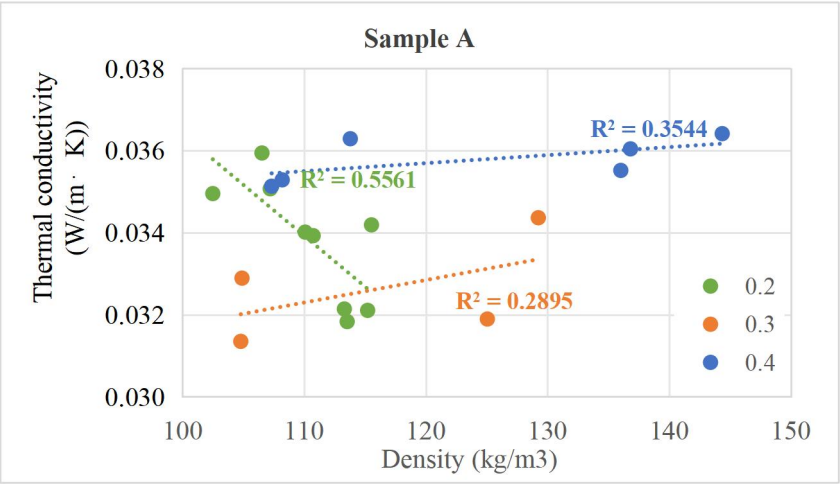

Figure 6. The density and thermal conductivity of sample A. The three differently colored dashed lines represent the linear regression fits for the three groups with different compression rates. R^2 value is the coefficient of determination that represents how well the linear regression model fits the data.

In Figure 6, a linear regression analysis was performed on the density and thermal conductivity of Sample A, grouped by different compression levels. Although the R^2 values for each group are not sufficient to establish a definitive linear relationship, the trend lines indicate distinct patterns. Specifically, Sample A shows a decrease in thermal conductivity as density increases after a minor compression of 20%. However, as the compression rate increases to 30% and 40%, the thermal conductivity begins to increase along with density. Similar trends are observed for Samples OB and B, as illustrated in Figure S1.

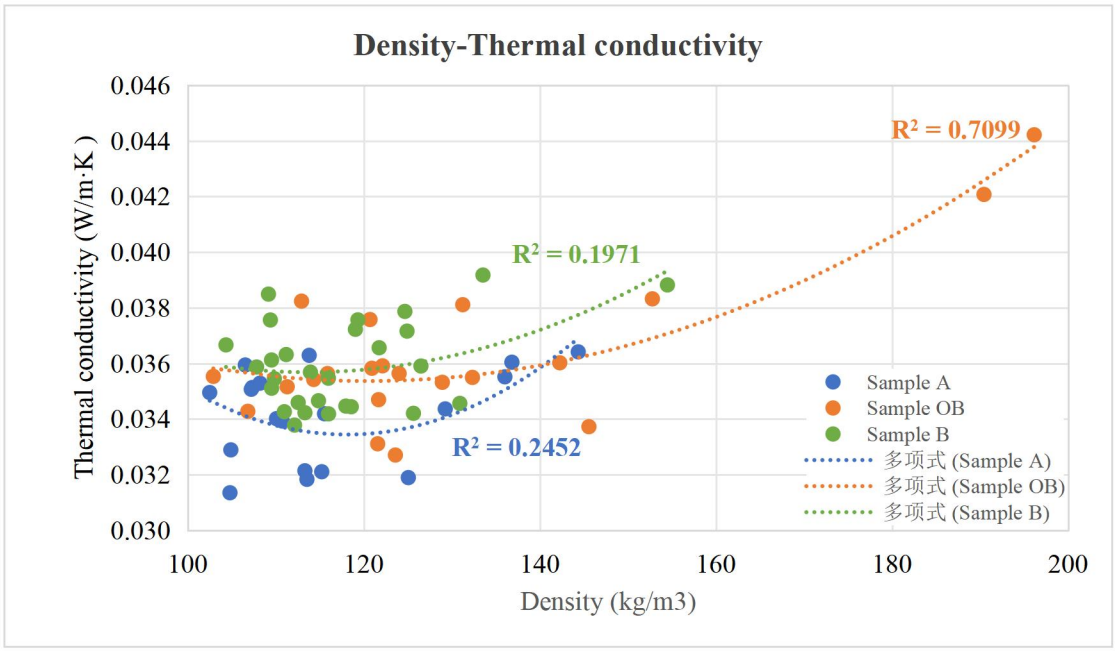

Figure 7. The density and thermal conductivity of all samples, including the three sample types and various compression groups. The three differently colored dashed lines represent the polynomial regression fits corresponding to each of the three sample types. R^2 value is the coefficient of

determination that represents how well the polynomial regression model fits the data.

When these results are considered alongside the earlier observation that the density of the samples increased statistically while thermal conductivity did not exhibit a statistically significant change, it is reasonable to hypothesize that the relationship between density and thermal conductivity in mycelium composites is not simply linear. Instead, thermal conductivity appears to decrease with increasing density up to a certain point, after which it begins to increase.

To further explore this hypothesis, polynomial regression was applied to the data for Samples A, OB, and B, as shown in Figure 7, rather than the linear regression used in Figure 5. The R^2 values of the polynomial fits for these three sample types are notably improved compared to those from the previous linear regression analysis. Notably, Sample OB achieved an R^2 value of 0.7099, indicating that the data aligns well with the polynomial regression model.

3.2.2. Rebound Rate – Compresstion rate

During the experiment, the length and width of the samples did not show significant changes, so the change in height before and after compression can be used to calculate the volume ratio before and after compression. According to the experimental data (Table 4), all mycelium composite samples demonstrated good rebound performance. By the third day after compression, the rebound height of the samples had stabilized. For some samples, measurements were continued for a month, and results indicated no trend of shrinkage; in fact, the height slightly increased compared to the height measured on the third day after compression. However, the density and thermal conductivity did not show significant changes, so the height measured on the third day was considered the final height for calculating the final rebound rate and the volume ratio V_2/V_0.

Table 4. Height changes and rebound rates of samples after different levels of compression. $Strain_1$ refers to the applied compression rate, calculated as the ratio of the compressed distance to the original height of the sample. h_0 denotes the original height of the samples before compression. h_1 is the height immediately after compression. h_2 was measured after a 3-day rest period to assess rebound, and h_3 was measured 30 days post-compression. V_2/V_0 represents the percentage of the original volume retained by the sample on the third day after compression.

Sample type	Groups		Height (cm)				Rebound rate %	V_2/V_0 %
	$Strain_1$ %	n	h_0	h_1	h_2	h_3		
A	20	3	10.00	8.00	8.93	9.13	46.67 ± 7.17	89.33
	30	2	10.00	7.00	8.20		40.00 ± 84.71	82.00
	40	3	9.88	6.05	7.68		45.00 ± 11.47	77.74
OB	20	3	10.00	8.00	9.13	9.30	56.67 ± 14.34	91.33

	30	3	10.00	7.00	8.33		44.44 ± 12.65	83.33
	50	2	10.00	5.00	6.75	6.90	35.00 ± 12.71	67.50
B	10	3	9.73	8.76	9.45		71.09 ± 16.64	97.09
	20	6	9.62	7.69	8.83		59.29 ± 5.05	91.85
	30	3	9.50	6.65	8.25		56.58 ± 35.68	86.84
	40	3	9.65	5.79	7.05		32.64 ± 2.89	73.06

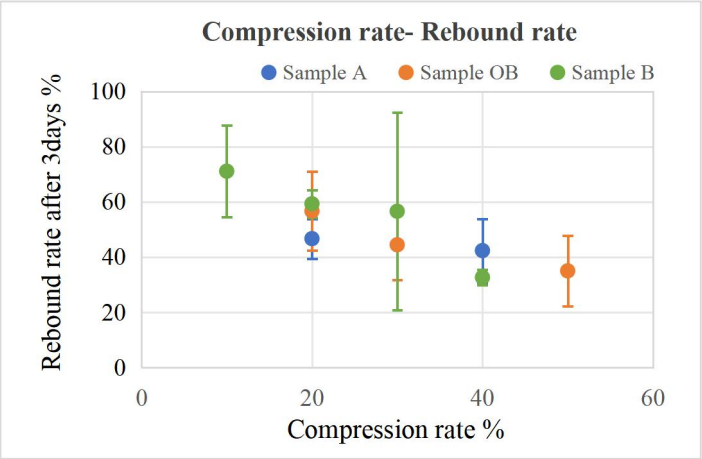

Figure 8. The rebound rate of samples with different compression rates. Error bars represent the 95% confidence interval (CI). The rebound rate of Sample A after 30% compression was excluded from the figure due to an excessively large CI.

Sample A, after being compressed by 20%, rebounded to 89.33% of its original volume by the third day, with a rebound rate of 46.67 ± 7.17%. This rebound performance was lower than that of samples OB and B under the same compression level, which had higher rebound rates of 56.67 ± 14.34% and 59.29 ± 5.05%, respectively. Table 4 and Figure 8 clearly show that the rebound rates for samples OB and B decrease as the compression rate increases. However, this trend was not observed for Sample A. Although the CI for the rebound rate of Sample A at 30% compression was too large to be considered reliable, the rebound rate of Sample A at 40% compression was 45.00 ± 11.47%. This rate was not significantly different from the rebound rate of Sample A at 20% compression, and it was significantly higher than that of Sample B at the same level of compression and even slightly higher than that of Sample OB at 30% compression. Therefore, it is possible that Sample A exhibits more stable rebound performance across different compression levels.

3.3. Compressive strength measurement

Due to time constraints, compressive strength measurements were conducted on only a subset of samples, as detailed in Table 5. These samples were from the manual compression experiment, where they were subjected to varying compression levels, allowed to rebound. This compressive strength test was intended to assess how

different precompression levels affect the samples' mechanical properties.

Table 5. Compressive Young's Modulus of Different Samples. The following samples are from the previous manual compression experiment. The samples were first compressed and allowed to rebound before undergoing compressive testing to evaluate their mechanical properties.

Sample type	Samples	n	Compression rate %	Young's modulus (MPa)
A	A2	3	20	1.30 ± 0.24
B	B0	2	0	0.55 ± 0.10
	B1	3	10	0.55 ± 0.08
	B2	3	20	1.26 ± 0.12
	B3	3	30	1.20 ± 0.95
OB	OB2	3	20	1.08 ± 0.28
	OB3	3	30	1.27 ± 0.55

Young's modulus, which indicates material rigidity, was also assessed. Among the tested samples, Sample A with 20% compression exhibited the highest Young's modulus at 1.30 ± 0.24 MPa, surpassing even Sample B and OB after 30% compression. This suggests that Sample A with 20% compression is the strongest of the samples tested. For Sample B, there was no significant difference in Young's modulus between the uncompressed sample and the sample compressed by 10%. However, after 20% compression, Young's modulus more than doubled compared to both the uncompressed sample and the sample with 10% compression.

4. Discussion

4.1. Thermal testing by HFM-100 and TEMPOS

Rockwool and EPS are commonly used thermal insulation materials. Rockwool has a thermal conductivity ranging from 0.033 to 0.050 W/m·K, with a density between 20 and 200 kg/m³, while EPS has a thermal conductivity of 0.035 to 0.040 W/m·K and a density of 15 to 35 kg/m³ or more (Danaci & Akin, 2022; Hung Anh & Pásztory, 2021). When comparing the thermal conductivity of these two insulation materials measured by the HFM-100 and the TEMPOS with their known values, it is evident that the HFM-100 provides more accurate results.

The thermal conductivity values of Sample A (0.0542 W/m·K) and Sample B (0.0539–0.0666 W/m·K) measured by the HFM-100 are significantly higher than the target thermal conductivity of 0.038 W/m·K. These values also exceed those of commonly used insulating materials, such as glass wool and rock wool, and are notably higher than polyurethane (PUR) (0.024–0.03 W/m·K) and polyisocyanurate (PIR) (0.018–0.028 W/m·K). Therefore, the thermal insulation performance of the material requires further optimization.

Despite that the HFM-100 is more reliable for thermal test, the TEMPOS was chosen for this research for several reasons. First, the minimum sample dimensions required for the HFM-100 are 15 cm in width and length, but the largest sample size used in the manual compression experiment was 10 x 10 x 10 cm, constrained by the 10 x 10 cm inner size of the metal container. Second, each test with the HFM-100 takes around 1 to 2 hours, which is time-consuming and did not align with the research schedule. In contrast, a single round of testing with the TEMPOS, including three repetitions for one sample, requires only about 35 minutes. Furthermore, the primary goal of the manual compression experiment was to compare thermal conductivity before and after various levels of compression rather than to determine the exact thermal conductivity. As long as the same testing device was used throughout the experiment, the data remained comparable. Additionally, the thermal conductivity values measured by the TEMPOS were consistently lower than those measured by the HFM-100, but there was a strong linear relationship between the results from both devices. This indicates a stable difference attributable to different calculation methods or testing processes, rather than any failure of the TEMPOS. For uncompressed materials, the HFM-100 provided more accurate thermal conductivity measurements. For small-sized samples that had undergone compression, the thermal conductivity could be reasonably estimated using the data obtained from the TEMPOS and the linear regression formula derived from the comparison.

4.2. The relationship between density and thermal conductivity

From the results of density and thermal conductivity measurements on various mycelium composites, which were subjected to compression rates ranging from 10% to 50%, some key observations were made. When the material was compressed to a smaller degree, such as 10% or 20% of its original volume, the density increased after the material rebounded. However, the thermal conductivity tended to decrease. Moreover, data analysis revealed that for most samples, even though the density significantly increases after compression, the thermal conductivity does not show a statistically significant change. This led to the hypothesis that the thermal conductivity of mycelium composites appears to initially decrease and then increase as density rises with greater compression rates.

In an attempt to support this hypothesis, relevant studies from previous research were reviewed. Veiseh et al. (2009) developed a mathematical model for the relationship between density and thermal conductivity across a broad density range for fiber insulation materials. As shown in Figure 10, the thermal conductivity of rock wool (Figure 9.a) and glass wool (Figure 9.b) decreases to a minimum point as density increases, and then it begins to rise. The polynomial fitting of the data collected in this research also exhibited a similar trend. However, further research is needed to reinforce these findings. Increasing the number of samples and expanding the density range of the material will be essential to constructing a more persuasive and accurate mathematical model, akin to that shown in Figure 9. Such a model would provide valuable insights for better standardizing the production specifications of mycelium-based materials.

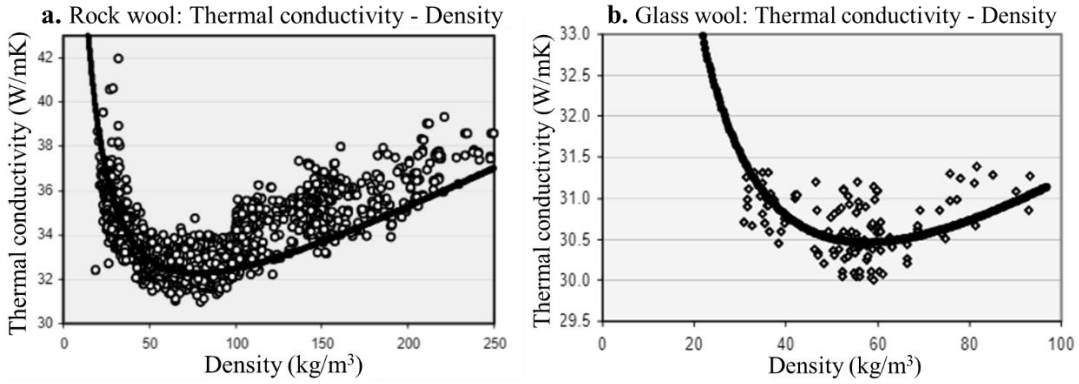

Figure 9. The relationship between density and thermal conductivity of rock wool (a) and glass wool (b). Images are from (Veiseh, Khodabandeh, & Hakkaki-Fard, 2009)

What is the underlying cause of the observed trend in which the thermal conductivity of fibrous materials, including mycelium composites, first decreases and then increases with changes in density? This section aims to explore this question in detail.

Materials with good thermal insulation properties typically have low density and high porosity. Porosity, which refers to the proportion of voids within a material relative to its total volume, is a crucial factor determining the thermal performance of fibrous materials (Xiong et al., 2021).Air has a relatively low thermal conductivity of 0.026-0.068 W/m·K at 27°C to 627°C (Graczykowski et al., 2017).Theoretically, air is a better insulator compared to the wood fibers (0.04 - 0.09 W/m·K at 30°C - 270°C) and grass fibers (0.033-0.04 W/m·K at -4°C-350°C) used in our mycelium composites (Hung Anh & Pásztory, 2021). When the thermal conductivity of the solid matrix is higher than that of the gas within the material, increasing porosity leads to more air being trapped within the material, thereby reducing the overall thermal conductivity and enhancing its insulation properties (Liu & Zhao, 2022; Sun, Hu, Li, Zhang, & Sun, 2014).

In addition to porosity, pore size also significantly influences the thermal insulation properties of materials. The effective thermal conductivity of porous materials results from the combined effects of heat conduction through the solid matrix and gas molecules within the pores ($kcond$), convective heat transfer within the pores ($kconv$), and infrared thermal radiation ($krad$) (Liu & Zhao, 2022).When the diameter of the air pockets within the material exceeds 4 mm, the air has sufficient space to move, leading to heat convection and consequently increasing the material's overall thermal conductivity. Therefore, the thermal insulation performance of a material is closely related not only to its porosity but also to the size of the pores. Increasing porosity while reducing pore size can effectively enhance the thermal insulation properties of porous fibrous materials (Xiong et al., 2021).

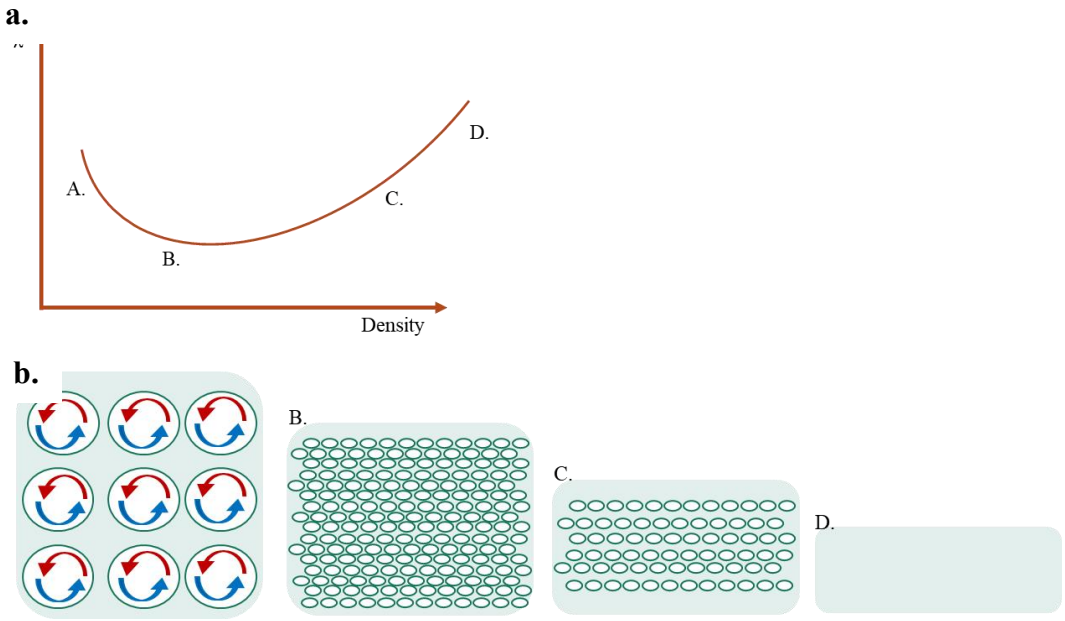

Figure 10. A proposed model illustrating the potential variation in thermal conductivity with changes in density during the compression of mycelium composites. Graph (a) presents a simplified trend curve depicting the relationship between thermal conductivity and density. Panel (b) hypothesizes

the internal structural states of the material corresponding to the key points on the trend curve.

Figure 10 illustrates a hypothesized model based on the above principles, which explains the variation in thermal conductivity with changes in density as mycelium composites are compressed. In Figure 10.b, point A represents the uncompressed, original mycelium composite, which contains large air pockets due to uneven material formation. These large air pockets facilitate convective heat transfer, corresponding to point A in Figure 10.a. When the material undergoes mild compression to 90% or 80% of its original volume, a small amount of air is expelled, reducing porosity. However, the large pores are likely compressed into smaller, more enclosed spaces, effectively trapping the air and reducing convective heat transfer. This state, labeled as B, is characterized by a high porosity with smaller pore sizes, resulting in lower thermal conductivity compared to state A.

Our previous data analysis indicated that, for most samples, even though density significantly increases after compression, thermal conductivity does not show a statistically significant change. This scenario might correspond to the material being compressed directly from state A to state C. In state C, although the pores are smaller, the substantial expulsion of air leads to a significant reduction in porosity, causing thermal conductivity to rise to a level similar to that in state A. As compression continues to state D, nearly all the air might be expelled, and the solid fibrous matrix becomes overly compressed, leading to higher thermal conductivity and a substantial decline in insulation performance.

This finding is highly beneficial for the development of our Cir-Q product. If we can further establish a comprehensive mathematical model describing the relationship between thermal conductivity and density under compression, it would be possible to produce mycelium composites at the A point and then compress them to achieve the optimal B point within the OSB.

4.3. Optimal compression rate

The primary objective of this study was to determine the optimal compression level for the mycelium-based filling in Cir-Q materials, ensuring a perfect fit within the OSB cases without gaps and maximizing thermal insulation. The selection of the most suitable candidate was evaluated by considering thermal insulation performance, rebound rate, and compressive strength. Since the primary function of the product is insulation, thermal performance was the dominant criterion in this selection process. The rebound performance was also crucial, as it not only helps to prevent gaps but also potentially reduces material costs. Additionally, although mycelium composites are primarily intended as insulation materials, sufficient material strength is a bonus, especially for applications in walls, floors, or roofing.

Based on our experimental and analytical findings, Sample A compressed by 20% and

allowed to rebound naturally, exhibited the lowest thermal conductivity among all samples. After being compressed to 80% of its original volume, Sample A recovered 89.3% of its original volume by the third day and remained stable. Although this rebound rate is slightly lower than Sample B's 91.9%, the difference is not statistically significant. Furthermore, Young's modulus of Sample A after 20% compression was the highest among all tested samples. Therefore, compressing Sample A by 20% emerged as the optimal strategy in this study.

Under this optimal strategy, if the internal height of the OSB cases is 20 cm, the mycelium filling should be cut to a thickness of around 22.39 cm. When compressed by 20% and placed inside the OSB, the filling would rebound to make seamless contact with the OSB, while maintaining or even enhancing its thermal insulation properties compared to the uncompressed mycelium filling.

4.4. The quality of mycelium composites

During this study, it was observed that the quality of the mycelium composites provided by FC-i was inconsistent. Specifically, these materials exhibited significant heterogeneity. As shown in Figure 11, the substrate particles within the composites were unevenly distributed, with some areas containing large chunks of wood fiber (Figure 11.a). Additionally, the internal colonization of the mycelium was inconsistent, leading to the formation of voids (Figure 11.b). In some cases, cutting the material revealed large holes where the substrate had disintegrated (Figure 11.c). These issues likely stem from excessive internal temperatures during the growth process or inadequate oxygen supply (Elsacker, Søndergaard, Van Wylick, Peeters, & De Laet, 2021), resulting in mycelium inactivation and incomplete colonization. These voids are certain to impact both the thermal insulation and mechanical properties of the mycelium composites (Dias et al., 2021) (Dias et al., 2021).

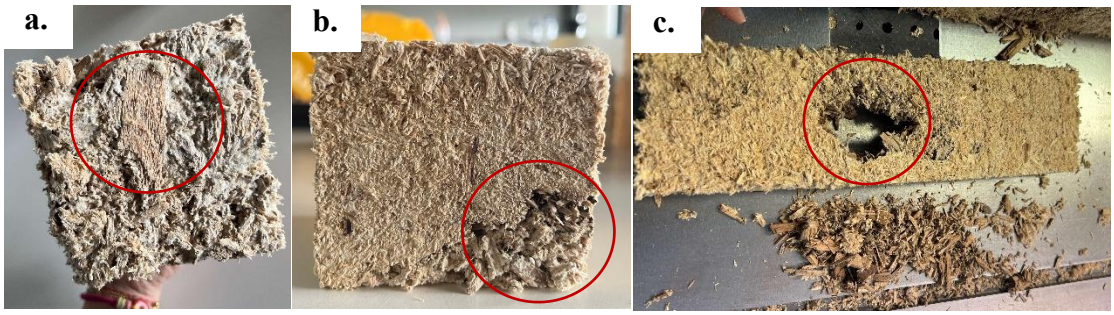

Figure 11. Examples of lower-quality mycelium composites. (a) Large substrate particles; (b) Uncolonized substrate; (c) Big uncolonized area in the middle of the material.

These inconsistencies presented challenges during the experimental process. First, the high rejection rate of the cut mycelium composite samples limited the number of usable samples, reducing the number of replicates available for testing. This, in turn, impacted the accuracy of the experimental data. In the manual compression test,

samples with visibly uneven colonization, such as those shown in Figure 11.b, could be easily identified and discarded. However, some samples had poorly colonized areas located internally, making them difficult to detect. When these samples were used in the manual compression test, uneven rebound was observed, complicating data collection and reducing accuracy. This inconsistency was also reflected in the larger CI observed in the mean values of certain measurements.

In terms of thermal testing, the material's heterogeneity was also evident. For example, two samples of Sample B, taken from the same batch of material, showed significant differences in thermal conductivity when measured using the HFM-100, with values of 0.0539 W/m·K and 0.0666 W/m·K. Additionally, during thermal conductivity measurements with the TEMPOS system, it was apparent that certain areas of the same sample were more loosely packed and easier to insert the probe into, while other areas were denser and more resistant, making probe insertion difficult. The variability in measurements from different locations within the same sample often necessitated additional measurements to minimize random errors, but this also increased the time required for testing.

4.5. Further research and suggestions

Based on the opportunities and challenges discussed above, several recommendations for future research directions are proposed.

- Developing a complete mathematical model of the relationship between density and thermal conductivity of mycelium composites:

During the manual compression experiments, an intriguing observation was made: slight compression led to a decrease in thermal conductivity, suggesting that mycelium ccomposites may exhibit a trend where thermal conductivity initially decreases and then increases with increasing density. This finding is highly advantageous for the development of Cir-Q products. To build upon this, it is recommended to extend the compression-rebound-thermal conductivity testing. This involves increasing the scale of compression, expanding the density range, increasing the sample size, and employing more precise automated compression instruments. Such measures will provide a comprehensive dataset to construct a robust mathematical model describing the relationship between density and thermal conductivity of mycelium ccomposites. Verifying this hypothesis could significantly benefit the standardization of mycelium material production. In the future, it may be possible to produce mycelium composites with specific densities, compress them by 20% for put in OSB cases, and achieve optimal thermal performance upon rebound, ensuring a seamless fit with the OSB.

- Optimizing Mycelium Composite Formulations:

Addressing the challenge of improving the insulation performance of mycelium composites is crucial. It is advisable to begin by adjusting the ratios of the components in the current substrate formulation and enhancing the uniformity of substrate particle size. Additionally, exploring alternative substrates, such as hemp shives, which are locally produced in the Netherlands and commonly used in mycelium composites production (Schmidt et al., 2023; Zimele et al., 2020), could be beneficial. Cattail, with its unique porous sponge-like structure, may also have potential as a substrate. Furthermore, experimenting with different fungal species, such as *Trametes versicolor* (M. Zhang, Zhang, et al., 2023), *Fomes fomentarius* (Schmidt et al., 2023) and *Pleurotus ostreatus* (Alemu, Tafesse, & Mondal, 2022), or even co-cultivating two fungal strains, could yield improvements in material properties.

- Measuring and Optimizing Porosity:

Increasing material porosity while reducing pore size can significantly enhance insulation performance. Utilizing scanning electron microscopy (SEM) to evaluate the microstructural formation of mycelium composites (Dias et al., 2021)will allow for detailed analysis of porosity and pore size. By acquiring precise information about the porosity and pore structure of the produced mycelium materials, adjustments can be made to substrate formulations or particle sizes, thereby optimizing thermal insulation performance.

- Enhancing Production Processes:

A significant challenge in scaling up mycelium materials for construction applications is the inadequate colonization due to oxygen deficiency within the material. Research by Elsacker et al. (2021) provides a reference approach involving the layered production of mycelium composite pannels. Multiple layers of mycelium composites are stacked and then self-welded into a single, cohesive material through the natural growth of the mycelium. Subsequently, these mycelium blocks are cut into specific structures using digitally controlled robotic wire-cutting machine. Another research used a similar modular production strategy, utilizing the bio-welding ability of living mycelium to bridge gaps and connect modular mycelium blocks to achieve material scales unattainable with molds alone(McBee et al., 2022). However, this may increase the demand for larger drying equipment. Future research could also explore symbiosis with oxygen-producing algae (Elsacker et al., 2021) or bacteria that generate oxygen in dark environments (Ettwig et al., 2012) to improve mycelium material production.

5. Conclusion

This study presents several promising findings and opportunities for the further development of Cir-Q products.

Firstly, all mycelium composite samples demonstrated excellent rebound properties, particularly when subjected to mild compression of 10% or 20%. The materials were able to rebound to 90%–97% of their original volume in a short period and remained stable, with no observed tendency to shrink over time. This outcome alleviates concerns about the potential for poor rebound or shrinkage in the mycelium fillings within OSB cases.

Secondly, it was observed that mild compression of the mycelium composites (10% or 20%) resulted in a slight reduction in thermal conductivity. This phenomenon may be attributed to a maintained porosity while the pore size decreases, leading to improved thermal insulation. Further analysis revealed a trend in which the thermal conductivity of the mycelium composites initially decreases, reaching a minimum point, and then begins to increase as density continues to rise. Developing an accurate data model that correlates density and thermal conductivity for these composites in future research would be highly beneficial for the standardized production of Cir-Q mycelium fillings.

Considering thermal insulation performance, rebound capacity, and compressive strength, compressing Sample A by 20% emerged as the optimal strategy in this study. Experimental and analytical results showed that Sample A, after being compressed by 20% and allowed to rebound naturally, exhibited the lowest thermal conductivity, the highest compressive Young's modulus, and a favorable rebound rate among all tested samples.

The saw-then-compress method is promising in its potential to prevent thermal bridging, as the mycelium fillings, upon rebounding from compression, make seamless contact with the OSB. Additionally, if the compression rate is well-controlled, the thermal insulation of the material could even be enhanced post-compression.

Besides of these positive findings, There are still some remaining challenges such as optimal the substrat recipe and innovating production strategy to futher improving the thermal insulation performance to get the aimed thermal conductivity of 0.038 W/m·K.

Reference

Alemu, D., Tafesse, M., & Mondal, A. K. (2022). Mycelium-Based Composite: The Future Sustainable Biomaterial. *2022*(1), 8401528. doi:https://doi.org/10.1155/2022/8401528

Angelova, G. V., Brazkova, M. S., & Krastanov, A. I. (2021). Renewable mycelium based composite - sustainable approach for lignocellulose waste recovery and alternative to synthetic materials - a review. *Z Naturforsch C J Biosci, 76*(11-12), 431-442. doi:10.1515/znc-2021-0040

Antinori, M. E., Ceseracciu, L., Mancini, G., Heredia-Guerrero, J. A., & Athanassiou, A. (2020). Fine-Tuning of Physicochemical Properties and Growth Dynamics of Mycelium-Based Materials. *ACS Appl Bio Mater, 3*(2), 1044-1051. doi:10.1021/acsabm.9b01031

Bitting, S., Derme, T., Lee, J., Van Mele, T., Dillenburger, B., & Block, P. (2022). Challenges and Opportunities in Scaling up Architectural Applications of Mycelium-Based Materials with Digital Fabrication. *Biomimetics (Basel), 7*(2). doi:10.3390/biomimetics7020044

Danaci, H. M., & Akin, N. (2022). Thermal insulation materials in architecture: a comparative test study with aerogel and rock wool. *Environmental Science and Pollution Research, 29*(48), 72979-72990. doi:10.1007/s11356-022-20927-2

Dias, P. P., Jayasinghe, L. B., & Waldmann, D. (2021). Investigation of Mycelium-Miscanthus composites as building insulation material. *Results in Materials, 10*, 100189. doi:https://doi.org/10.1016/j.rinma.2021.100189

Elsacker, E., Søndergaard, A., Van Wylick, A., Peeters, E., & De Laet, L. (2021). Growing living and multifunctional mycelium composites for large-scale formwork applications using robotic abrasive wire-cutting. *Construction and Building Materials, 283*, 122732. doi:https://doi.org/10.1016/j.conbuildmat.2021.122732

Ettwig, K. F., Speth, D. R., Reimann, J., Wu, M. L., Jetten, M. S. M., & Keltjens, J. T. (2012). Bacterial oxygen production in the dark. *3*. doi:10.3389/fmicb.2012.00273

FC-Insulation. (2021). FC-insulation producer of Biological insulation materials for the building industry. Circular insulation material. Retrieved from https://fc-i.com/en/

Girometta, C., Picco, A., Baiguera, R., Dondi, D., Babbini, S., Cartabia, M., . . . Savino, E. (2019). Physico-Mechanical and Thermodynamic Properties of Mycelium-Based Biocomposites: A Review. *Sustainability, 11*. doi:10.3390/su11010281

Graczykowski, B., El Sachat, A., Reparaz, J. S., Sledzinska, M., Wagner, M. R., Chavez-Angel, E., . . . Sotomayor Torres, C. M. (2017). Thermal conductivity and air-mediated losses in periodic porous silicon membranes at high temperatures. *Nature Communications, 8*(1), 415. doi:10.1038/s41467-017-00115-4

Hung Anh, L. D., & Pásztory, Z. (2021). An overview of factors influencing thermal conductivity of building insulation materials. *Journal of Building Engineering, 44*, 102604. doi:https://doi.org/10.1016/j.jobe.2021.102604

Jones, M., Mautner, A., Luenco, S., Bismarck, A., & John, S. (2020). Engineered mycelium composite construction materials from fungal biorefineries: A critical review. *Materials & Design, 187*, 108397. doi:https://doi.org/10.1016/j.matdes.2019.108397

Liu, H., & Zhao, X. (2022). Thermal Conductivity Analysis of High Porosity Structures with Open and Closed Pores. *International Journal of Heat and Mass Transfer, 183*, 122089. doi:https://doi.org/10.1016/j.ijheatmasstransfer.2021.122089

McBee, R. M., Lucht, M., Mukhitov, N., Richardson, M., Srinivasan, T., Meng, D., . . . Wang, H. H. (2022). Engineering living and regenerative fungal–bacterial biocomposite structures. *Nature Materials, 21*(4), 471-478. doi:10.1038/s41563-021-01123-y

Schmidt, B., Freidank-Pohl, C., Zillessen, J., Stelzer, L., Guitar, T. N., Lühr, C., . . . Meyer, V. (2023). Mechanical, physical and thermal properties of composite materials produced with the basidiomycete Fomes fomentarius. *Fungal Biology and Biotechnology, 10*(1), 22. doi:10.1186/s40694-023-00169-8

Sun, J., Hu, Z., Li, J., Zhang, H., & Sun, C. J. C. I. (2014). Thermal and mechanical properties of fibrous zirconia ceramics with ultra-high porosity. *40*(8), 11787-11793.

Sutcu, M. (2015). Influence of expanded vermiculite on physical properties and thermal conductivity of clay bricks. *Ceramics International, 41*(2, Part B), 2819-2827. doi:https://doi.org/10.1016/j.ceramint.2014.10.102

van den Brandhof, J. G., & Wösten, H. A. B. (2022). Risk assessment of fungal materials. *Fungal Biol Biotechnol, 9*(1), 3. doi:10.1186/s40694-022-00134-x

Veiseh, S., Khodabandeh, N., & Hakkaki-Fard, A. (2009). Mathematical models for thermal conductivity-density relationship in fibrous thermal insulations for practical applications. *Asian Journal of Civil Engineering, 10*.

Villasmil, W., Fischer, L. J., & Worlitschek, J. (2019). A review and evaluation of thermal insulation materials and methods for thermal energy storage systems. *Renewable and Sustainable Energy Reviews, 103*, 71-84. doi:https://doi.org/10.1016/j.rser.2018.12.040

Xiong, X., Venkataraman, M., Jašíková, D., Yang, T., Mishra, R., Militký, J., & Petrů, M. (2021). An experimental evaluation of convective heat transfer in multi-layered fibrous materials composed by different middle layer structures. *51*(3), 362-379. doi:10.1177/1528083719878845

Zhang, M., Xue, J., Zhang, R., Zhang, W., Peng, Y., Wang, M., & Cao, J. (2023). Mycelium Composite with Hierarchical Porous Structure for Thermal Management. *Small, 19*(46), 2302827. doi:https://doi.org/10.1002/smll.202302827

Zhang, M., Zhang, Z., Zhang, R., Peng, Y., Wang, M., & Cao, J. (2023). Lightweight, thermal insulation, hydrophobic mycelium composites with hierarchical porous structure: Design, manufacture and applications. *Composites Part B: Engineering, 266*, 111003. doi:https://doi.org/10.1016/j.compositesb.2023.111003

Zhang, X., Hu, J., Fan, X., & Yu, X. (2022). Naturally grown mycelium-composite as sustainable building insulation materials. *Journal of Cleaner Production, 342*, 130784. doi:https://doi.org/10.1016/j.jclepro.2022.130784

Zimele, Z., Irbe, I., Grinins, J., Bikovens, O., Verovkins, A., & Bajare, D. (2020). Novel Mycelium-Based Biocomposites (MBB) as Building Materials. *JOURNAL OF RENEWABLE MATERIALS, 8*, 1067-1076. doi:10.32604/jrm.2020.09646

Supplementary

Table S 1. Density thermal conductivity of samples before and after varying degrees of compression. *n* represents the number of repetitions in each group. *Strain 1* refers to the applied compressive strain, defined as the ratio of the compressed distance to the original height of the sample. ρ_0 and λ_0 denote the original density and thermal conductivity of the samples before compression. ρ_2 and λ_2 were measured after compression and a 3-day rest period for rebound. ρ_3 and λ_3 were measured 30 days after compression.

Sample type	Groups		Density (kg/m^3)			Thermal conductivity (W/(m·K))		
	Strain$_1$ %	n	ρ_0	ρ_2	ρ_3	λ_1	λ_2	λ_3
A	20	1	107.22	115.22	115.54	0.0351 ± 0.0051	0.0321 ± 0.0036	0.0342 ± 0.0023
		2	106.54	113.31	113.54	0.0359 ± 0.0025	0.0321 ± 0.0015	0.0318 ± 0.0006
		3	102.50	110.09	110.75	0.0350 ± 0.0021	0.0340 ± 0.0015	0.0339 ± 0.0034
	30	1	104.80	125.06		0.0314 ± 0.0033	0.0319 ± 0.0023	
		2	104.80	129.25		0.0329 ± 0.0043	0.0344 ± 0.0028	
	40	1	107.34	136.82		0.0351 ± 0.0010	0.0360 ± 0.0044	
		2	113.80	144.36		0.0363 ± 0.0033	0.0364 ± 0.0015	
		3	108.20	136.03		0.0353 ± 0.0037	0.0355 ± 0.0020	
OB	20	1	115.88	124.01	122.13	0.0356 ± 0.0029	0.0356 ± 0.0045	0.0359 ± 0.0063
		2	112.93	120.71	121.68	0.0382 ± 0.0015	0.0376 ± 0.0031	0.0347 ± 0.0039
		3	111.30	121.58	123.59	0.0352 ± 0.0053	0.0331 ± 0.0017	0.0327 ± 0.0017
	30	1	114.31	132.34		0.0354 ± 0.0053	0.0355 ± 0.0041	
		2	120.92	142.26		0.0358 ± 0.0045	0.0360 ± 0.0040	
		3	106.83	128.92		0.0343 ± 0.0051	0.0353 ± 0.0030	
	50	1	102.91	152.78	145.57	0.0355 ± 0.0030	0.0383 ± 0.0021	0.0337 ± 0.0014
		2	131.24	196.15	190.44	0.0381 ± 0.0015	0.0442 ± 0.0043	0.0421 ± 0.0050
B	10	1	109.52	110.98		0.0361 ± 0.0046	0.0343 ± 0.0036	
		2	109.17	112.55		0.0385 ± 0.0020	0.0346 ± 0.0017	
		3	104.35	109.84		0.0367 ± 0.0031	0.0355 ± 0.0013	
	20	1	117.96	124.67		0.0345 ± 0.0029	0.0379 ± 0.0085	
		2	118.58	126.49		0.0344 ± 0.0033	0.0359 ± 0.0019	
		3	112.14	125.64		0.0338 ± 0.0031	0.0342 ± 0.0030	
		4	107.83	115.98		0.0359 ± 0.0038	0.0355 ± 0.0032	
		5	116.00	130.91		0.0342 ± 0.0030	0.0346 ± 0.0033	
		6	114.85	121.74		0.0347 ± 0.0020	0.0366 ± 0.0017	
	30	1	109.39	133.54		0.0376 ± 0.0012	0.0392 ± 0.0024	
		2	109.53	119.05		0.0351 ± 0.0020	0.0372 ± 0.0030	
		3	113.32	124.91		0.0342 ± 0.0041	0.0372 ± 0.0017	
	40	1	113.94	154.49		0.0357 ± 0.0027	0.0388 ± 0.0060	
		2	111.19	152.55		0.0363 ± 0.0023	0.0376 ± 0.0036	
		3	119.33	160.85		0.0376 ± 0.0020	0.0391 ± 0.0040	

Table S 2. Height changes and rebound rates of samples after different levels of compression. $Strain_1$ refers to the applied compression rate, calculated as the ratio of the compressed distance to the original height of the sample. h_0 denotes the original height of the samples before compression. h_1 is the height immediately after compression. h_2 was measured after a 3-day rest period to assess rebound, and h_3 was measured 30 days post-compression. V_2/V_0 represents the percentage of the original volume retained by the sample on the third day after compression.

Sample type	Samples	Height (cm)				Compression rate %	Rebound rate %	V_2/V_0 %
		h_0	h_1	h_2	h_3			
A	2_1	10.00	8.00	8.90	9.10	20	45.00	89.00
	2_2	10.00	8.00	9.00	9.20	20	50.00	90.00
	2_3	10.00	8.00	8.90	9.10	20	45.00	89.00
	3_1	10.00	7.00	8.40		30	46.70	84.00
	3_2	10.00	7.00	8.00		30	33.30	80.00
	4_1	9.90	5.90	7.70		40	45.00	77.78
	4_2	10.00	6.00	7.80		40	45.0 0	78.00
	4_3	9.75	6.26	7.55		36	37.00	77.44
OB	2_1	10.00	8.00	9.20	9.40	20	60.00	92.00
	2_2	10.00	8.00	9.20	9.30	20	60.00	92.00
	2_3	10.00	8.00	9.00	9.20	20	50.00	90.00
	3_1	10.00	7.00	8.20		30	40.00	82.00
	3_2	10.00	7.00	8.50		30	50.00	85.00
	3_3	10.00	7.00	8.30		30	43.33	83.00
	5_1	10.00	5.00	6.80	7.00	50	36.00	68.00
	5_2	10.00	5.00	6.70	6.80	50	34.00	67.00
B	1_1	9.20	8.28	9.00		10	78.26	97.83
	1_2	10.00	9.00	9.70		10	70.00	97.00
	1_3	10.00	9.00	9.65		10	65.00	96.50
	2_1	9.30	7.44	8.60		20	62.37	92.47
	2_2	9.30	7.44	8.60		20	62.37	92.47
	2_3	9.50	7.60	8.60		20	52.63	90.53
	2_4	9.80	7.84	8.90		20	54.08	90.82
	2_5	10.00	8.00	9.20		20	60.00	92.00
	2_6	9.80	7.84	9.10		20	64.29	92.86
	3_1	10.00	7.00	8.20		30	40.00	82.00
	3_3	9.10	6.37	8.15		30	65.20	89.56
	3_4	9.40	6.58	8.40		30	64.54	89.36
	4_1	9.70	5.82	7.10		40	32.99	73.20
	4_2	9.65	5.79	7.00		40	31.35	72.54
	4_3	9.60	5.76	7.05		40	33.59	73.44

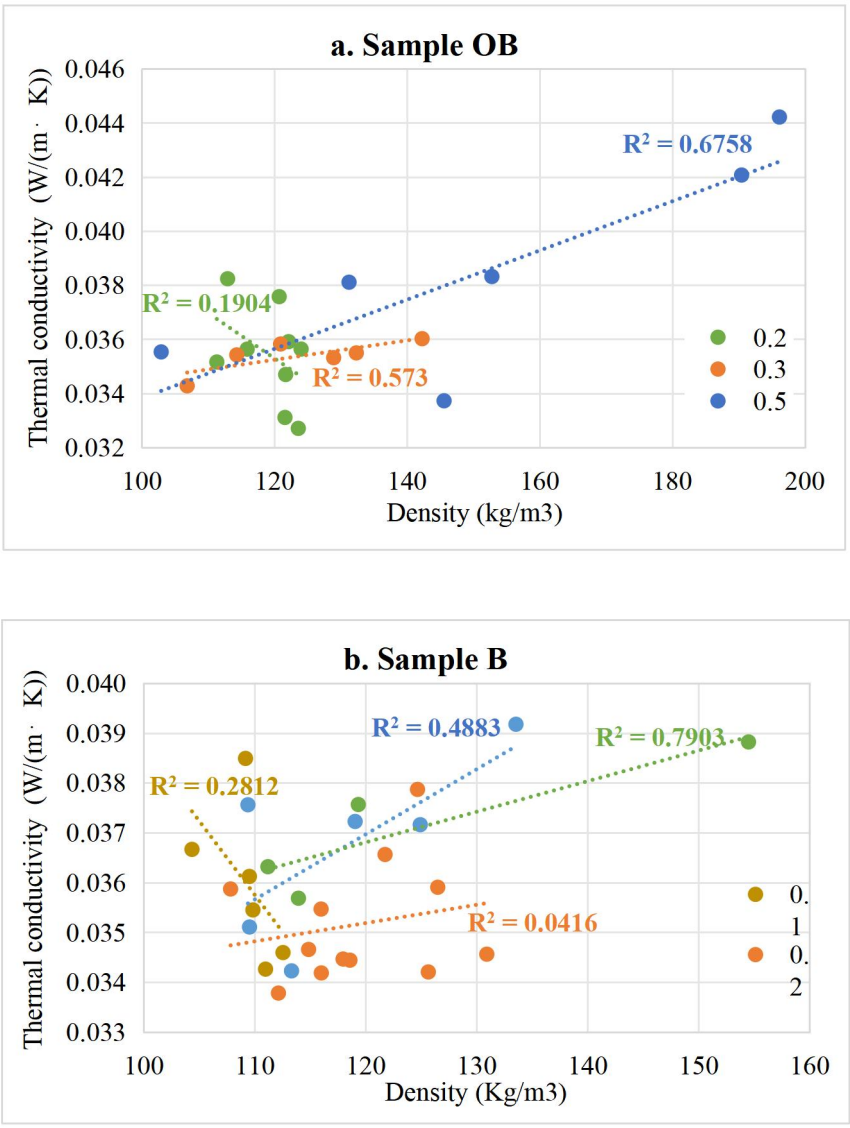

Figure S 1. The density and thermal conductivity of sample OB (a) and sample B (b). The three differently colored dashed lines represent the linear regression fits for the three groups with different compression rates. R^2 value is the coefficient of determination that represents how well the linear regression model fits the data.

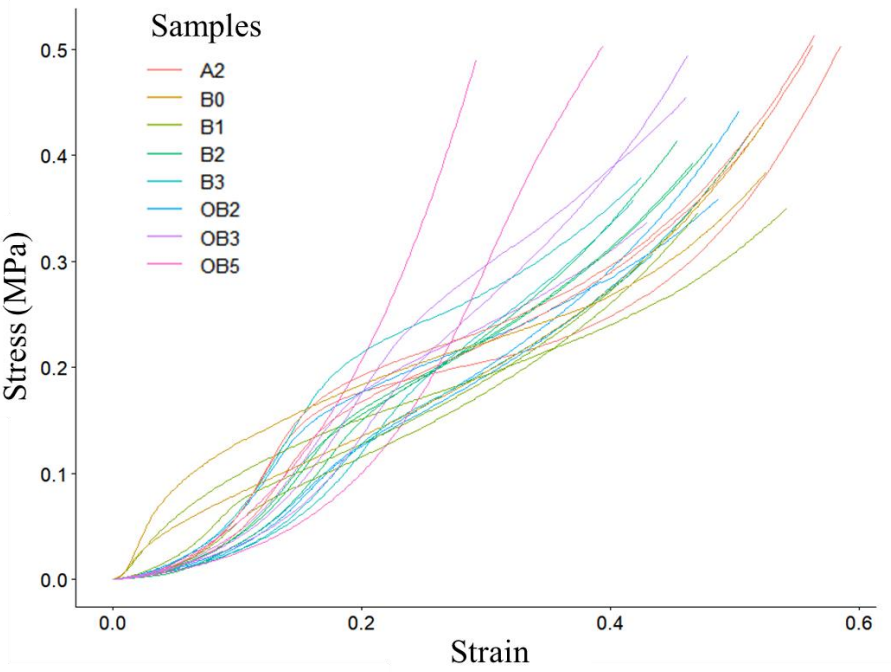

Figure S 2. The stress-strain curves obtained from compression testing of mycelium composite samples